



Erosion Behavior of Gelcast Fused Silica Ceramic Composites

Gurabvaiah Punugupati¹ · P. S. C. Bose¹ · G. Raghavendra¹ · C. S. P. Rao¹ · S. Ojha¹

Received: 4 April 2019 / Accepted: 10 May 2019 / Published online: 1 June 2019
© Springer Nature B.V. 2019

Abstract

In this paper, the characteristics of solid particle erosion on fused silica ceramics are investigated. Gelcasting, a near net shape forming process, is adopted for the fabrication of ceramics. Three types of ceramics with a combination of pure fused silica, fused silica+5 wt% silicon nitride (Si_3N_4) + 1 wt% boron nitride (BN) and fused silica+5 wt% silicon nitride (Si_3N_4) + 1 wt% alumina (Al_2O_3) are prepared at a constant 52 vol% solid loading, 10 wt% monomer content and 10:1 monomer ratio. Different impingement angles (30° , 45° , 60° and 90°) and three impact velocities (86 m/s, 101 m/s and 148 m/s) were chosen to examine the behavior of erosion on gelcasted ceramics using SiO_2 particles as erodent. The maximum rate of erosion is obtained at normal impingement angle (90°), which shows the brittle nature of ceramics. The impact velocity and angle of impingement have an appreciable effect on erosion rate. Resistance to erosive wear is found to have improved with the inclusion of reinforcements in the fused silica ceramics. The erosion rates of different ceramics are compared. Ceramic composite with a combination fused silica+5 wt% Si_3N_4 + 1 wt% BN shows the highest resistance to wear. The surface roughness and morphology of the eroded surfaces have also been studied.

Keywords Erosion · Gelcasting · Fused silica · Surface roughness

1 Introduction

Solid particle erosion (SPE) is illustrated as the ejection of material by the continuous impact of tiny erodent particles. The erosion phenomenon is useful under certain circumstances as in sand impacting and peak velocity abrasive water jet cutting but becomes a worrying factor when dealing with equipment like jet turbines, fluidized bed combustion system, pipe lines and valves carrying particulate matter, cyclone generators, gas turbines, burner parts and cutting tools. The directions of motion of solid particles contained in fluid (gaseous or liquid) medium can be accelerated or decelerated by fluid. SPE can be considered as abrasive erosion when the impact angle is between 0° to 30° and when impact erosion occurs for an impact angle between 60° to 90° [1–4].

Material loss happens by plastic misshapening or potentially brittle crack, contingent upon the material being dissolved or on

working factors. Ductile materials experience material loss from plastic distortion in which the material is evacuated by the dislodging or cutting activity of the disintegrating molecule. In brittle material, then again, the material is evacuated by the arrangement and convergence of cracks because of which grain discharge from outside the target material happens. Erosion in materials is based on many parameters like structure and characteristics of materials, exposure states, physical and chemical properties of erodent particles; which are interrelated [5–14]. The erosion behavior of brittle materials such as alumina ceramics, cermets has been examined earlier and it is observed that erosion is determined by the properties of both erodent and target material. Lidija curkovic et al. [1] experimentally examined the influence of hardness, shape of erodent and impingement angle on erosion of high purity alumina ceramics with two types of erodents viz. SiC and SiO_2 . It was found that hard and angular SiC particles had huge impact compared to delicate and rounded SiO_2 particles. Higher rate of erosion observed at normal impingement angle for both types of erodents. Hyeon-Ju Choi et al. [2] evaluated erosion characteristics of silicon nitride (Si_3N_4) ceramics. It has been observed that the erosion loss of ceramics depends on the grain size rather than hardness and fracture toughness (mechanical properties). Changxia Liu et al. [4] emphasized that erosion behavior is impacted by

✉ G. Raghavendra
raghavendra.gujjala@gmail.com

¹ Department of Mechanical Engineering, National Institute of Technology, Warangal, India

Table 1 Raw materials used for fabrication of ceramic composites

S. No.	Material	Function	Average particle size	Density (g/cm ³)	Supplier
1	Fused silica powder (SiO ₂)	Ceramic Powder	1–5 µm	2.2	M/S Ants Ceramics Pvt. Ltd., Thane, India
2	Silicon Nitride (Si ₃ N ₄)	Ceramic Powder	1–5 µm	3.44	M/S Ube Industries, Japan
3	Alumina (Al ₂ O ₃)	Ceramic Powder	50–200 µm	3.98	Alfa Aesar, USA
4	Methacrylamide CH ₂ -C(CH ₃)CONH ₂	Monomer		1.235	Sigma Aldrich Chemie, Germany
5	N N'-Methabisacrylamide (MBAM) (C ₇ H ₁₀ N ₂ O ₂)	Cross linker		1.24	Sigma Aldrich Chemie, Germany
6	Darvan 821A	Dispersant		1.25	Vanderbilt Minerals LLC, USA
7	Polyethylene glycol 400 (PEG-400) H(OCH ₂ CH ₂) _n OH	Surfactant		1.126	Sigma Aldrich Chemie, Germany
8	Tetramethylethylenediamine- (TEMED) C ₆ H ₁₆ N ₂	Catalyst		1.982	Sigma Aldrich Chemie, Germany
9	Ammonium persulfate (APS) H ₈ N ₂ O ₈ S ₂	Initiator		0.775	Alfa Aesar, USA
10	Diluted Nitric acid (HNO ₃) and Sodium hydroxide (NaOH)	pH adjustment			S. D. fine chemicals, India

impingement angle, impact velocity of erodent particles (SiC), phase ratio and relative density of boron carbide (B₄C) ceramic composites, fabricated using uniaxial hot pressing. Sandan Kumar Sharma et al. [15] experimentally investigated the influence of impingement angle with alumina and SiC as erodents on erosion characteristics of SiC-WC composites. G Amrithan

et al. [16] experimentally found the influence of particle size, impact velocity and impingement angle of erodent particles on erosion behavior of biomorphic Si/SiC ceramic composites. It is also found that erosion loss is very high when the impact angle is 90° when compared to the lower angles of incidence. Y. Zhang et al. [17] examined the rate of erosion of alumina

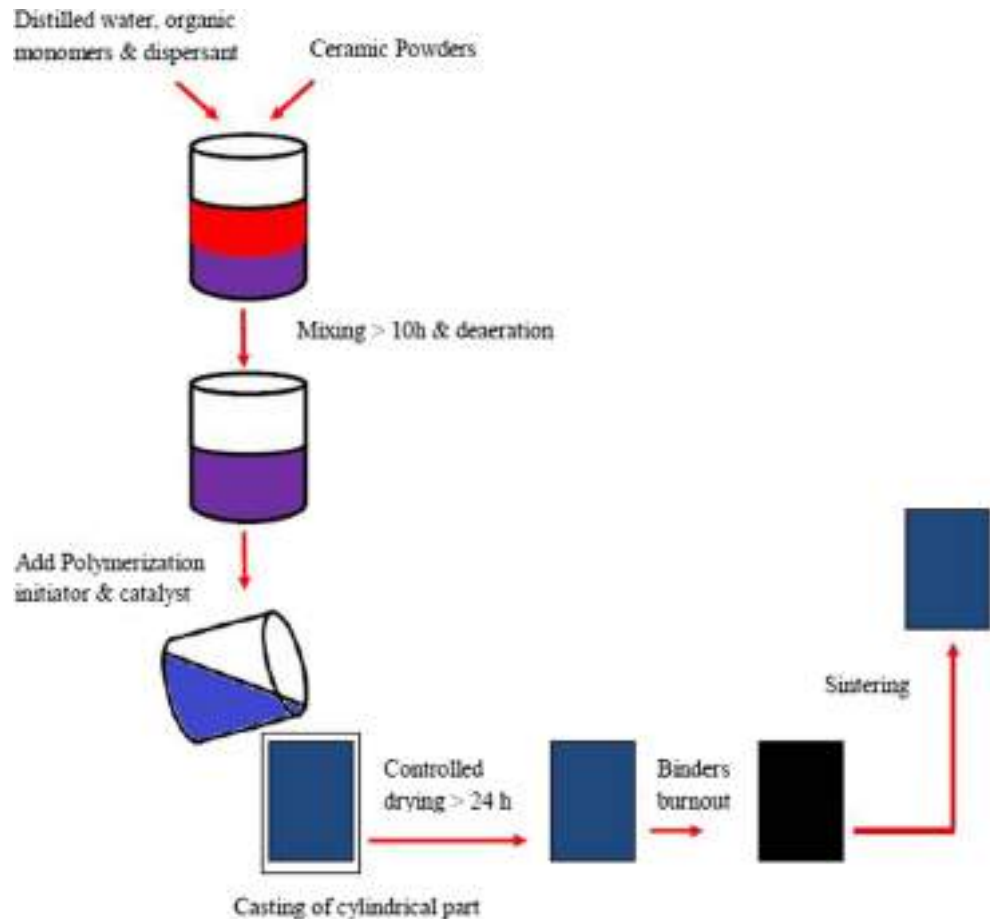
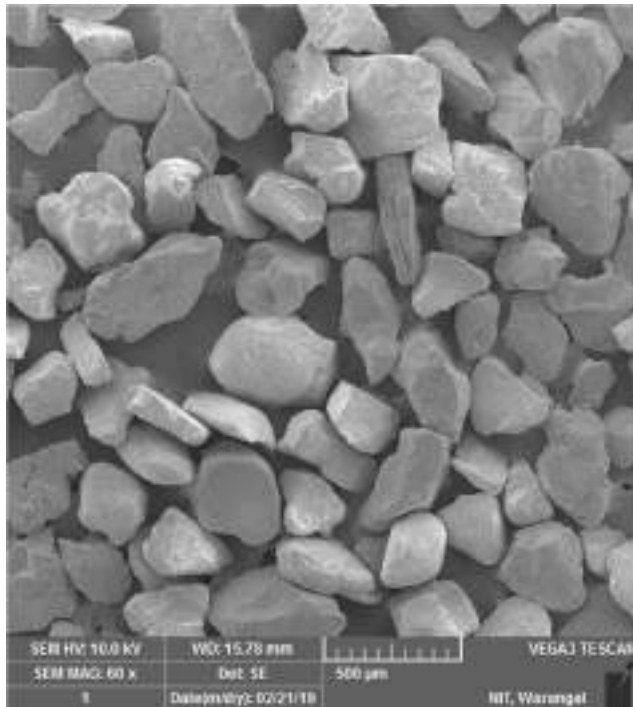
Fig. 1 Gelcast fabrication process flow chart

Table 2 Tested flexural strength and hardness (HV) of fused silica ceramic composites

S. No.	Sample	Flexural strength (MPa)	Hardness (HV)
1	Pure fused silica	43.2	482
2	Fused silica+5 wt% Si_3N_4 + 1 wt% BN	99.22	550
3	Fused silica+5 wt% Si_3N_4 + 1 wt% Al_2O_3	95.12	519

ceramics and found that it is enhanced with impact velocity of particles. The erosion rate for dry and wet erosion was obtained for different particle velocities and fluxes; being 37 m/s and 50 g/cm²sec for airborne erosion and 16.5 m/s and 120 g/cm²sec for slurry jet erosion. It is also observed that huge variation in erosion rates were found related to acute angles and normal impact. K. R. Gopi et al. [18] developed erosive wear models on the basis of experimental data which successfully validated most cited models in the literature. Erosion rate increases with increase in particle velocity for dry-impact erosion. A power law exponent which varies from 2.82 to 2.92 is obtained for velocity of particle. Erosion increases with sine of the angle of impact, with exponent ranging from 2.31 to 2.35 for dry-impact and 1.45 to 1.48 for slurry-impact respectively. Marijana Mjic renjo et al. [19] experimentally found erosion behavior and surface finish of slip cast Al_2O_3 - ZrO_2 ceramics with dry silica sand as erodent. The high temperature erosive loss of different materials such as SiC-WC composites [20], ZrB_2 -SiC composites [21], SiC- Si_3N_4 composite ceramic [22], reaction sintered Fe-Sialon ceramic composite [23], alumina ceramics [3] have also been studied.

**Fig. 2** SEM micrograph of silica erodent particles

Fused silica ceramics are attractive materials for many structural applications such as aerospace, insulators for electronics, antenna windows, and heat shields and for semiconductor manufacturing. These ceramics possess high chemical resistance, low thermal expansion co-efficient, good thermal shock resistance and excellent optical qualities [24, 25]. The main drawbacks of fused silica ceramics are low resistance to erosion and low mechanical strength for the use in radomes [26]. To overcome the drawbacks, reinforcements like Si_3N_4 [27], BN [28], Al_2O_3 [29] and graphene [30] were added to fused silica. Some literatures is available on the erosion studies of gelcast fused silica ceramics. Gelcasting, a novel ceramic manufacturing technique, is used to prepare ceramic composites; involving a simple casting process. The complex and complicated shapes used in many industries can be prepared by gelcasting process.

In the current study, fused silica is added to 5 wt% Si_3N_4 + 1 wt% BN and 5 wt% Si_3N_4 + 1 wt% Al_2O_3 to fabricate hybrid ceramic composites. Methacrylamide and Methabisacrylamide were used as monomer and cross linker respectively. The monomer content 10 Wt% and monomer ratio 10:1 were used at 52 vol% solid loading for the preparation of ceramics [24, 25]. The effects of impingement angle and impact velocity on erosion rate and surface roughness of pure fused silica, fused silica+5 wt% Si_3N_4 + 1 wt% BN and fused silica+5 wt% Si_3N_4 + 1 wt% Al_2O_3 ceramic composites were investigated.

2 Experimental

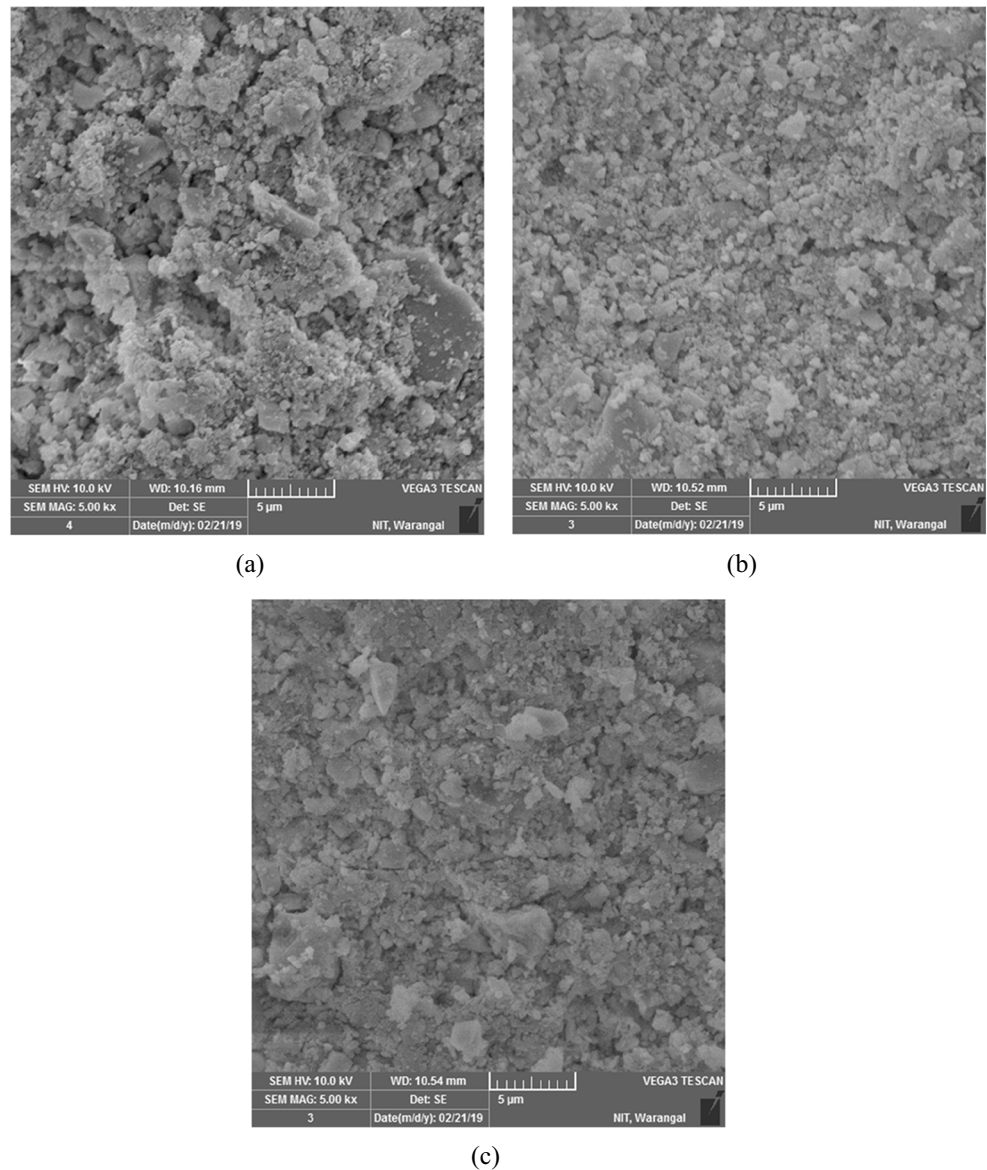
2.1 Characterization of Fused Silica Ceramic Composites

Solid particle erosion tests were performed on gelcast ceramic composites. The raw materials used for the current study are given in Table 1.

The ceramic composites were fabricated by gelcasting technique. The process flow chart of the gelcasting technique is shown in Fig. 1.

Ceramic composites were fabricated by considering 52 vol% solid loading, 10 wt% monomer content and 10:1 monomer ratio. Initially distilled water was added with dispersant Darvan 821A (1 wt% of MAM + MBAM), PEG (surfactant), monomers (10 wt% of SiO_2) and ceramic powders. The premix blend was then mixed using magnetic stirrer for more than 6 h. Deaerator was used to remove the dissolved air

Fig. 3 SEM images of fused silica ceramics **(a)** pure fused silica **(b)** fused silica+5 wt% Si_3N_4 + 1 wt% BN **(c)** fused silica+5 wt% Si_3N_4 + 1 wt% Al_2O_3



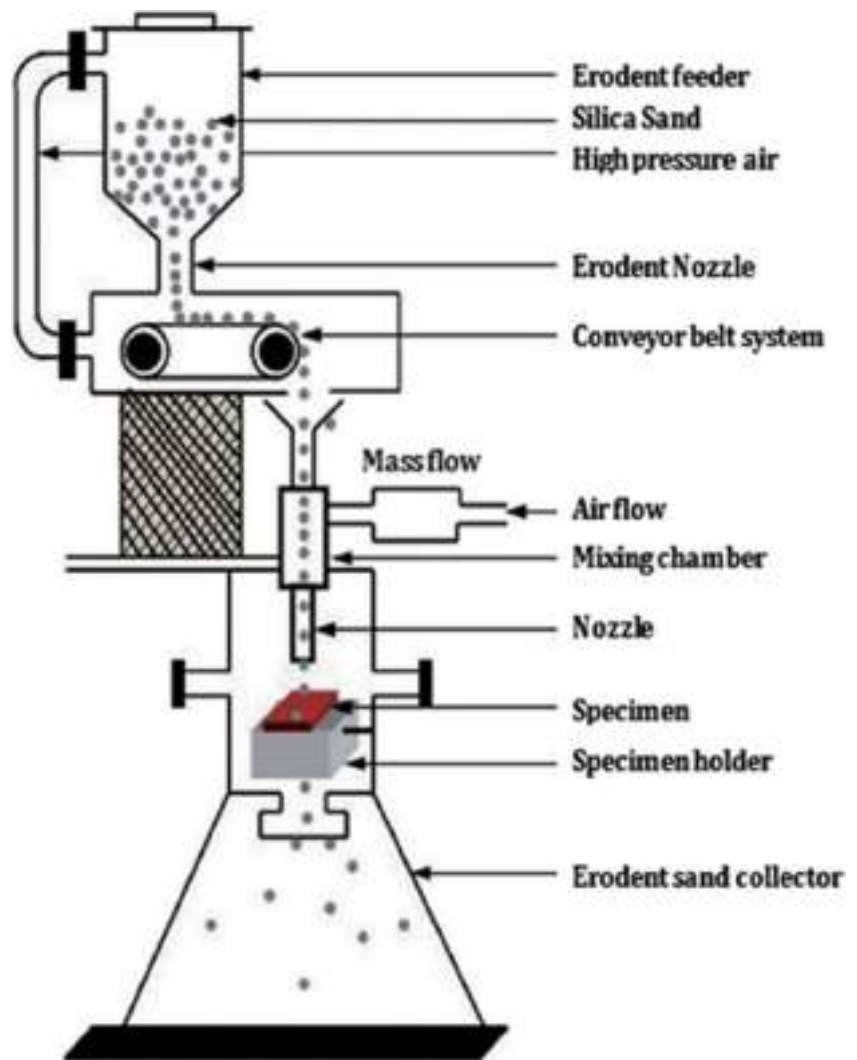
particles from slurry. APS and TEMED were added to the slurry to start polymerization and solidification. Then the solution was poured into gas mold and after polymerization, the green bodies were molded. Green samples were dried in a controlled temperature and humidity heater for 20 h. Later, binders were burnt at a temperature of 600 °C for 2 h with a heating rate of 4 °C/min and followed by pressure less sintering at 1250 °C for 1 h under nitrogen atmosphere. The sintered specimens were sliced into 3x4x40 mm³ size to conduct 3- point bending test to determine the flexural strength; according to ASTM (C1161–94) standard. The hardness of ceramic composites was found using Vickers hardness

method. Ceramic surface was examined using Diamond indenter. An average of 20 impressions were made on entire specimen using a load of 9.80 N for 10 s. The tested flexural strength and hardness of fused silica ceramic samples are given in Table 2.

The SEM micro graph of the used erodent is shown in Fig. 2. It is observed that particles have angular shape with average particle size of $200 \pm 20 \mu\text{m}$.

The microstructure of the three ceramic specimens was observed using scanning electron micro scope (SEM) on polished and thermally etched surfaces presented in Fig. 3.

Fig. 4 Schematic diagram of erosion test rig [31]



2.2 Erosion Wear Testing

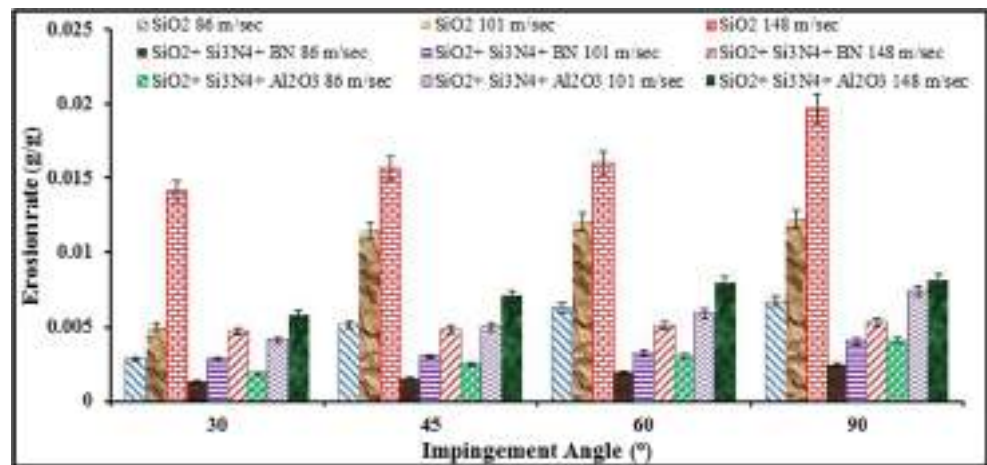
Fused silica ceramic composite specimens were polished to obtain fine surface finish. Then, samples were cleaned

ultrasonically in alcohol and dried at 100 ± 5 °C for 2 to 4 h. Erosive wear experiment was performed at room temperature on erosion test rig as per ASTM G76 standard. The outline sketch of the erosion test is presented in Fig. 4 [31].

Table 3 Process parameters for erosion test

S. No.	Test conditions	
1	Erodent type	Silica sand
2	Sample size	20x20x5 mm ³
3	Erodent particle size (μm)	200 ± 20
4	Erodent shape	Angular
5	Hardness of erodent (HV)	1420 ± 50
6	Impact angles (α°)	30, 45, 60 and 90
7	Impact velocity (m/s)	86, 101 and 148
8	Feed rate of erodent (g/min)	2 ± 0.02
9	Experimental temperature	Room Temperature (RT)
10	Standoff distance from Nozzle to sample (mm)	10 ± 1

Fig. 5 Erosion rate of ceramics with impingement angle at impact velocities 86 m/s, 101 m/s and 148 m/s



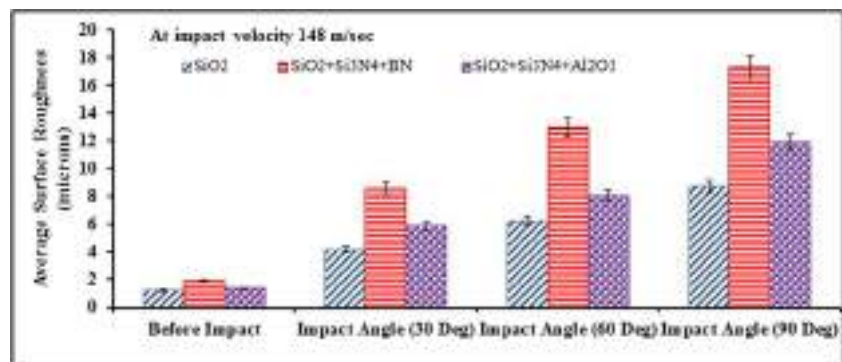
The erosion test rig contains air compressor, a conveyor or belt type particle feeder which controls the amount of sand particles and air mixing and acceleration chamber. The compressed air provides necessary pressure to the chosen range of silica sand which is pumped constantly by a conveyor belt feeder into the mixing chamber. This pressurized air then passes through a convergent brass nozzle with internal diameter of 3 mm. The specimen is impinged by erodent particles at various angles which can be controlled by a swivel head and an adjustable sample holder [32]. The experimental conditions for the solid particle erosion test are presented in Table 3.

The ceramic samples were weighed before and after the erosion test with the help of an electronic weigh balance of accuracy ± 0.01 mg. The amount of weight loss was found by measuring the loss of ceramic samples. The same procedure was continued until the erosion rate reached a stable condition. The erosion rate was calculated using Eq. 1.

$$\text{Erosion rate } (E_r) = \frac{\Delta m_1}{\Delta m_2} \quad (1)$$

Where, Δm_1 = weight loss of ceramic composite and Δm_2 = total weight of erodent particles.

Fig. 6 Surface roughness of ceramics at different impingement angle and at impact velocity of 148 m/s



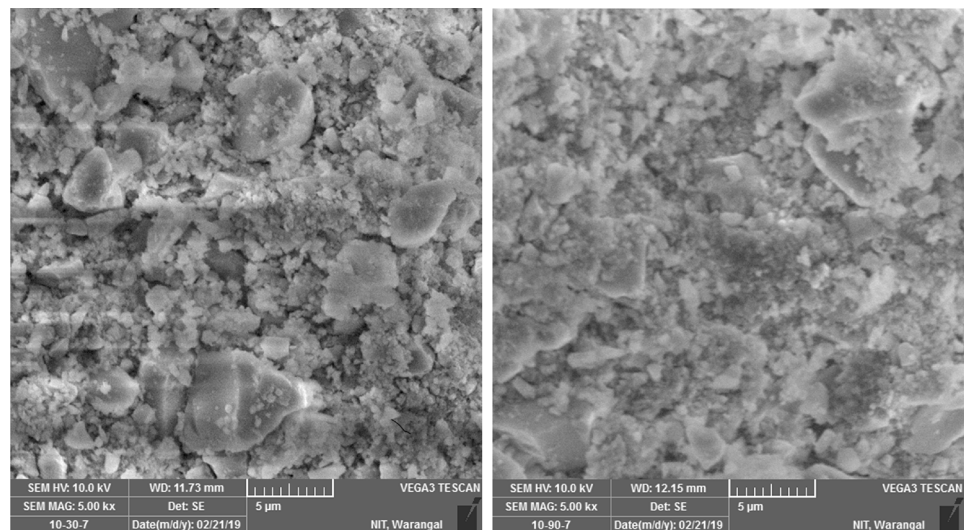
Additional accurate data was procured by surface roughness measurements and by analyzing the eroded surface using profilometer and SEM, respectively. The surface roughness of ceramic specimens was measured before and after erosion test using Taylor Hobson profilometer. The eroded surfaces were examined by SEM (VEGA 3LMU, TESCAN, Czech Republic).

3 Results and Discussion

Figure 5 shows the erosion rate of fused silica ceramic composites variation with impingement angle and impact velocity. Erosive wear resistance depends on the properties of the target material, erodent type, size, test conditions, equipment, environment and set tribological system [1]. The materials are mainly characterized as ductile and brittle based on erosive studies. The maximum erosion rate of ductile materials like metals occurs at low impact angles of 15° – 30° , whereas for brittle materials such as ceramics, it happens at or near normal impingement angle i.e. 90° .

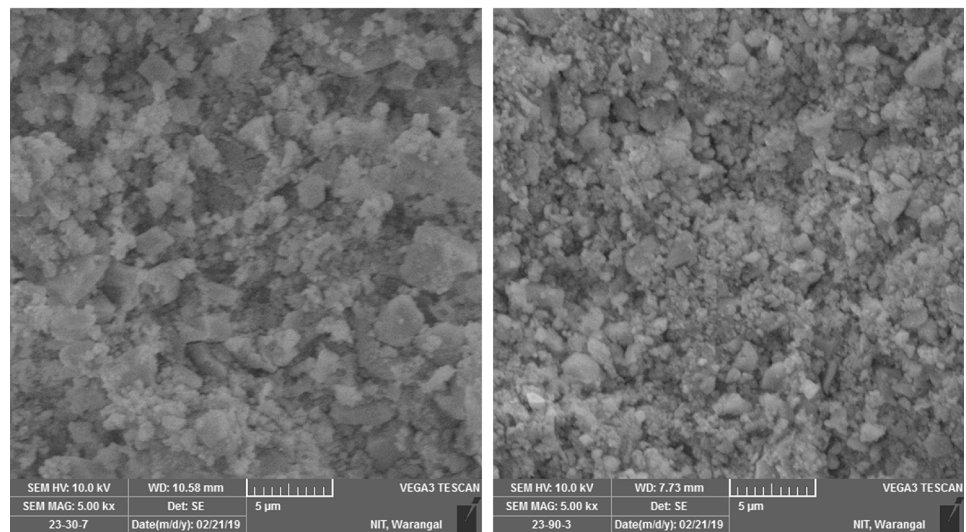
From Fig. 5, it is found that erosion rate of all three fused silica ceramics increases with impingement angle

Fig. 7 SEM micrographs of eroded surfaces **(a)** Pure fused silica at 30° impact angle **(b)** Pure fused silica at 90° impact angle **(c)** Fused silica+5 wt% Si_3N_4 +1 wt% BN at 30° impact angle **(d)** Fused silica+5 wt% Si_3N_4 +1 wt% BN at 90° impact angle **(e)** Fused silica+5 wt% Si_3N_4 +1 wt% Al_2O_3 at 30° impact angle **(f)** Fused silica+5 wt% Si_3N_4 +1 wt% Al_2O_3 at 30° impact angle



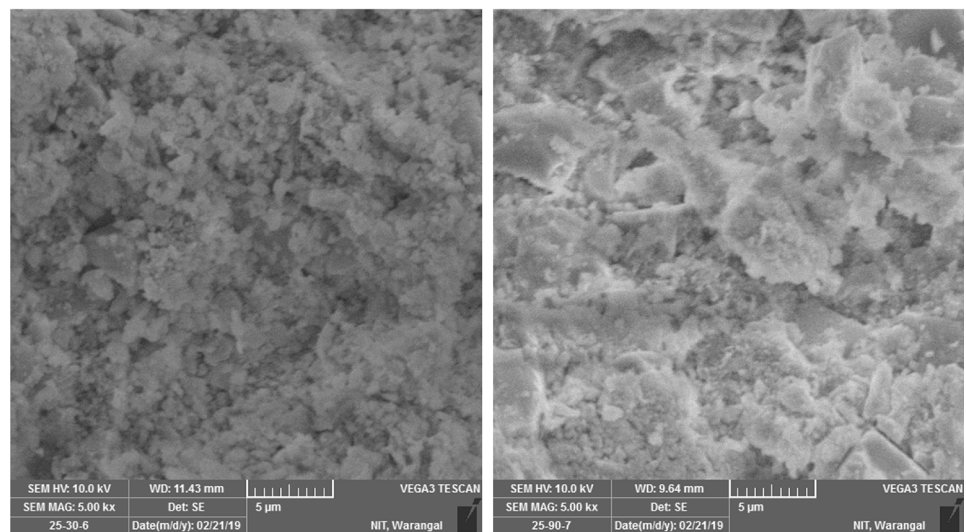
(a)

(b)



(c)

(d)



(e)

(f)

and impact velocity. Higher erosion rate happened at normal impingement angle for all specimens. Moreover, erosion rate was more at higher impact velocities. It is evident that erosion rate is based on impingement angle and impact velocity of erodent particles. Solid erosive wear loss is higher for pure fused silica compared to combined ceramic composites. The order of erosion rate is maximum for pure fused silica followed by fused silica+5 wt% Si_3N_4 + 1 wt% BN and fused silica+5 wt% Si_3N_4 + 1 wt% Al_2O_3 .

The flexural strength of the pure fused silica ceramics is low compared to the remaining ceramic composites, as evident from Table 2. Moreover, the erosion rate of 5 wt% Si_3N_4 + 1 wt% BN and fused silica is low compared to fused silica+5 wt% Si_3N_4 + 1 wt% Al_2O_3 for any given angle of impact and impingement velocity. The strength and hardness of the BN ceramics is relatively more in comparison with Al_2O_3 ceramics.

Surface roughness values were measured before and after the erosion tests with impact angles of 30°, 60° and 90° respectively using Taylor Hobson profilometer. The selected range of measuring surface roughness values was obtained and presented based on weight loss results i.e. minimum wear rate (30° impact angle) and maximum wear rate (normal impact angle) at higher impingement velocity.

The average surface roughness (Ra) values were obtained from these measurements. Variations of surface roughness with impact angle for different ceramics are shown in Fig. 6.

Surface roughness is more for eroded surfaces compared to un-eroded surfaces. It is observed that the surface roughness is more at normal impingement compared to acute impact angle. The morphology of the surfaces after erosion test (at impingement angles 30° and 90°) at impact velocity 148 m/s are presented in Fig. 7.

A comparison is drawn between the eroded specimen surface of silica ceramic composites at impingement angles of 30° and 90° at impact velocity 148 m/s. Grain ejection was prime material removal mechanism but it led to low plastic deformation when the impingement angle was close to normal impact; on the other hand, ploughing mechanism was dominant in the case of acute impingement angles. The ploughing mechanism is related to plastic smearing and removal of the surface material. The hardness of the ceramic material opposes plastic deformation, so that the erosion rate is low at low impingement angles. At normal impacts close to 90°, the erosion rate is more because of low fracture toughness and hardness which results in cracks that grow to form a crack network across the grain boundaries. These findings are in agreement with previous studies on erosion mechanisms on ceramics [1, 19]. In order to analyze the damages and erosion mechanisms, the structure of the eroded surfaces of the specimen was examined by SEM.

It is reported that bulk materials like ceramics are indeed influenced by erosion mechanism i.e. ratio of

particle hardness to target ceramic hardness (H_p/H_t). When the ratio (H_p/H_t) is >1 , wear mechanism essentially includes the indentation induced fracture. For lower ratios, such cracking is curbed and the material removal takes place by less critical microchipping mechanism. In the case of erosion studies of fused silica ceramics (target-t) with silica erodents (particles-p), the H_p/H_t ratio for pure fused silica, fused silica+5 wt% Si_3N_4 + 1 wt% BN and fused silica+5 wt% Si_3N_4 + 1 wt% Al_2O_3 are 0.334, 0.387 and 0.365 respectively.

4 Conclusions

Gelcasted ceramics with combinations of pure fused silica, fused silica+5 wt% Si_3N_4 + 1 wt% BN and fused silica+5 wt% Si_3N_4 + 1 wt% Al_2O_3 were used to perform solid particle erosion test at room temperature using SiO_2 particles as erodent. Erosion behavior of gelcasted fused silica ceramics as a function of impingement angle (30°, 45°, 60° and 90°) and impact velocities (86 m/s, 101 m/s and 148 m/s) was examined. The following major conclusions are drawn.

- The erosive wear rate of fused silica ceramics is a function of composition of ceramic, impact velocity and impingement angle. It is examined in general that erosion rate enhances with impact velocity and impingement angle. It was examined that higher erosion rate occurs at near normal impingement angle i.e. 90°.
- Erosion rate is maximum for pure fused silica ceramic compared with silica based ceramic composites. This may be attributed to the influence of hardness of ceramics.
- Morphology of the eroded surface is mainly based on the size and shape of erodent particles. The average surface roughness of eroded ceramics is more compared to un-eroded surfaces. Moreover, surface roughness increases from acute impingement angles to normal impingement angles. The ascending order of surface roughness values of ceramics is as follows

(i) fused silica+5 wt% Si_3N_4 + 1 wt% BN, (ii) fused silica+5 wt% Si_3N_4 + 1 wt% Al_2O_3 and (iii) pure fused silica.

References

1. Curkovic L et al (2011) Solid particle erosion behaviour of high purity alumina ceramics. *Ceram Int* 37:29–35
2. Choi HJ, Han DH, Park DS, Kim HD, Han BD, Lim DS, Kim IS (2003) Erosion characteristics of silicon nitride ceramics. *Ceram Int* 29:713–719

3. Wang X, Fang M, Zhang LC, Ding H, Liu YG, Huang Z, Huang S, Yang J (2013) Solid particle erosion of alumina ceramics at elevated temperature. *Mater Chem Phys* 139:765–769
4. Liu C, Sun J (2010) Erosion behaviour of B₄C-based ceramic composites. *Ceram Int* 36:1297–1302
5. Muruges L, Scattergood RO (1991) Effect of erodent properties on the erosion of alumina. *J Mater Sci* 26:5456–5466
6. Srinivasan S, Scattergood RO (1988) Effect of erodent hardness on erosion of brittle materials. *Wear* 128:139–152
7. Shipway PH, Hutchings IM (1996) The role of particle properties in the erosion of brittle materials. *Wear* 193:105–113
8. Zhou J, Bahadur S (1991) The effect of material composition and operational variables on the erosion of alumina ceramics. *Wear* 150:343–354
9. Lathabai S, Pender DC (1995) Microstructural influence in slurry erosion of ceramics. *Wear* 189:122–135
10. Xiong F et al (1997) Effect of grain size and test configuration on the wear behavior of alumina. *J Am Ceram Soc* 80(5):1310–1312
11. Hussainova I (2001) Some aspects of solid particle erosion of cermets. *Tribol Int* 34:89–93
12. Celotta DW, Qureshi UA, Stepanov EV, Goulet DP, Hunter J, Buckberry CH, Hill R, Sherikar SV, Moshrefi-Torbati M, Wood RJK (2007) Sand erosion testing of novel compositions of hard ceramics. *Wear* 263:278–283
13. Hussainova I (2003) Effect of microstructure on the erosive wear of titanium carbide-based cermets. *Wear* 255:121–128
14. Hussainova I (2005) Microstructure and erosive wear in ceramic-based composites. *Wear* 258:357–365
15. Sharma SK, Kumar BVM, Lim KY, Kim YW, Nath SK (2014) Erosion behavior of SiC–WC composites. *Ceram Int* 40:6829–6839
16. Amirthan G, Udayakumar A, Bhanu Prasad VV, Balasubramanian M (2010) Solid particle erosion studies on biomorphic Si/SiC ceramic composites. *Wear* 268:145–152
17. Zhang Y, Cheng YB, Lathabai S (2000) Erosion of alumina ceramics by air- and water-suspended garnet particles. *Wear* 240:40–51
18. Gopi KR, Nagarajan R, Rao SS, Mandal S (2008) Erosion model on alumina ceramics: a retrospection, validation and refinement. *Wear* 264:211–218
19. Renjo MM, Ćurković L, Grilec K (2015) Erosion resistance of slip cast composite Al₂O₃–ZrO₂ ceramics. *Procedia Eng* 100:1133–1140
20. Sharma SK, Venkata Manoj Kumar B, Kim YW (2017) Effect of impingement angle and WC content on high temperature erosion behavior of SiC–WC composites. *Int J Refract Met H* 68:166–171
21. Sharma SK et al (2017) High temperature erosion behavior of spark plasma sintered ZrB₂–SiC composites. *Ceram Int* 43:8982–8988
22. Li X, Ding H, Huang Z, Fang M, Liu B, Liu Y, Wu X, Chen S (2014) Solid particle erosion-wear behavior of SiC–Si₃N₄ composite ceramic at elevated temperature. *Ceram Int* 40:16201–16207
23. Yang JZ, Huang ZH, Fang MH, Hu XZ, Liu YG, Sun HR (2013) Reaction sintered Fe–sialon ceramic composite: processing, characterization and high temperature erosion wear behavior. *J Asian Ceram Soc* 1:163–169
24. Kandi KK et al (2016) Effect of monomers content and their ratio on Gelcasting of fused silica. *T Indian Ceram Soc* 75(3):1–4
25. Punugupati G, Bose PSC, Raghavendra G, Rao CSP (2018) Influence of solid loading and ratio of monomers on mechanical and dielectric properties of hybrid ceramic composites. *Silicon*. <https://doi.org/10.1007/s12633-018-0061-4>
26. Kouroupis KB (1992) Flight capabilities of high-speed-missile radome materials. *Johns Hopkins APL Tech Dig* 13(3):386–392
27. Du H et al (2010) Effect of temperature on dielectric properties of Si₃N₄/SiO₂ composite and silica ceramic. *J Alloys Compd* 503:L9–L13
28. Jia D, Zhou L, Yang Z, Duan X, Zhou Y (2011) Effect of preforming process and starting fused SiO₂ particle size on microstructure and mechanical properties of pressurelessly sintered BN_p/SiO₂ ceramic composites. *J Am Ceram Soc* 94(10):3552–3560
29. Wan W et al (2016) Effect of trace alumina on mechanical, dielectric, and ablation properties of fused silica ceramics. *J Alloys Compd* 675:64–72
30. Chen B, Liu X, Zhao X, Wang Z, Wang L, Jiang W, Li J (2014) Preparation and properties of reduced graphene oxide/fused silica composites. *Carbon* 77:66–75
31. Latha PS et al (2015) Evaluation of mechanical and tribological properties of bamboo–glass hybrid fiber reinforced polymer composite. *J Ind Text*:1528083715569376
32. Panchal M, Raghavendra G, Prakash MO, Ojha S (2018) Effects of environmental conditions on erosion wear of eggshell particulate epoxy composites. *Silicon* 10:627–634

Publisher's Note Springer Nature remains neutral with regard to jurisdictional claims in published maps and institutional affiliations.